COMPOSITE PIEZOELECTRICS FOR ULTRASONIC TRANSDUCERS

W. Wersing

Siemens AG, Corporate Research and Development, Munich, FRG

Abstract

Composite piezoelectrics are very interesting as transducers for future medical devices. This paper compares the properties of ceramic-plastic composites and of porous ceramics with various structures of pores with each other. The emphasis lies on those properties that are important for the mentioned application. The properties of porous ceramics were calculated based on Bruggemann's theory, those of regularly structured composites were calculated with a cell model. Here, the discussion is restricted to the case where the composite can be considered as being a homogeneous medium. The results for the calculations agree well with the known measured values. It is shown that within all the treated composite classes one can find materials with a sufficiently high coupling factor (≈0.5), a low lateral coupling factor, a low quality factor (≈15), and a low acoustical impedance (≈$8 \cdot 10^6$ kg/m^{2}s). Composites with very fine internal structure are best suited for the application in ultrasonic antennas. Several production techniques are discussed. Among these, the photolithographic methods offer interesting possibilities for the preparation of composites.

1. Introduction

Today, piezoelectric ceramics are generally used as transducer material in medical diagnosis instruments having ultrasonic antennas which function according to the pulse echo principle. These ceramics offer a number of advantages such as

1. an efficient conversion of electrical into mechanical energy and vice versa by their high electromechanical coupling ($k_t \approx 0.4$-0.5)
2. the possibility of varying the ceramic's permittivity for the electrical adaption to the electronics in a wide range
3. sufficiently low mechanical ($Q > 10$) and dielectrical ($\tan\delta < 0.05$) losses to achieve a high sensitivity.

On the other hand, they also have decisive disadvantages. Most problematic is their high acoustical impedance ($Z \approx 30 \cdot 10^6$ kg/m^{2}s), making at least 2 adaption layers necessary for a sufficient broad-band adaption to human tissue. In addition, the mechanical quality factors of most ceramics with values of $Q_m \approx 50$ are not low enough to allow the highest possible bandwidth or the shortest possible pulse and therefore the best lateral resolution. Since the individual array elements are usually wider than they are thick, the elements produce low frequent transverse vibrations which might also be transmitted. Due to the much lower absorbtion of low frequent sound waves in tissue, a noticeable reduction in image quality is caused and artefacts might be produced [1]. In modern arrays, these disturbing transverse vibrations are suppressed through a mechanical division (sash sawing) of the individual elements into subelements with a width to thickness ratio < 1.

For transducers for high frequencies or with complicated geometry (e.g. annular array), this technique of sash sawing becomes increasingly difficult. Thus, one tries to find piezoelectric materials which make it possible to dispense with this technique and which also do not possess the other disadvantages of piezoelectric ceramics.

Piezoelectric plastics (PVF_2) do not have the negative properties of ceramics. However, because of their low electromechanic coupling and their high dielectric losses, their sensitivity is very limited. it is also very difficult to adapt them electrically to the electronics because of their low permittivity.

Since the properties of multiphase material do not depend solely on the type and portion of volume of the individual phases but also on their interconnection*, this brings about a new dimension for optimizing material [2]. Even with the combination of only two phases, such as piezoelectric ceramic and plastic, a number of piezoelectric composites can be produced [3]. If one of the material phases is air, one normally speaks of porous ceramics. Their properties can, however, also be described well within the same framework as composites [4].

The demands on the structural properties of composites which are to be used in ultrasonic image screens will be discussed in the following. Then, the relevant properties of various composites will be theoretically determined, compared with one another, and their experimental confirmation will be discussed. Finally, processes of preparing suitable composites will be presented.

2. Composites for Medical Applications

As was described in the introduction, the usefulness of a piezoelectric composite depends, on the one hand, on its type of microstructure, i.e. its connectivity, on the other hand, on the fine detail of its structure.

CH2358-0/86/0000-0212 $1.00

A finely divided ultrasonic array can be viewed as a ceramiplastic composite with connectivity 2-2**. Comparison of this with the connectivity pattern given by Newnham [2] should show similar properties as those of composites with connectivity 2-0, 1-0, 1-1, 1-2, 1-3. Since the interconnection of the plastic phase is insignificant, the simple structures 2-2 and 1-3 can be applied. Figure 1, left, shows a sketch of a composite with 1-3 connectivity. Properties, production techniques and application of composites with 1-3 connectivity were extensively researched in recent years [6,7,16-19]. These composites have become an attractive material for medical ultrasonic transducers. In addition, porous piezoelectric ceramics with 3-3 and 3-0 connectivity possess piezoelectric properties that are quite interesting for these applications [4].

If a composite possesses a periodic microstructure (period **a**), the dimension of this microstructure, i.e. the size of **a** plays an important role. As soon as the wavenumber of laterally moving waves (Lamb waves) is a multiple of π / **a** , stop bands occur in the Lamb wave dispersion relation. These cause disturbing resonances in the response behavior of the composite. These effects were studied in detail for composites with 1-3 connectivity - in theory by Wang et al. [5] and in experiment by Gururaja et al. [6]. They found that a composite vibrates at its thickness resonance frequency as a homogeneous body if the transverse wavelength in the plastic at this frequency is much greater than **a** ($\lambda_p >>$ **a**). Since the transverse sound velocity in the plastic is about half of the value of the longitudinal sound velocity in the composite, this means that **a** must be much smaller than the composite thickness (**a** $<< t_c$). Under these circumstances, the acoustical impedance of the composite is independent of frequency, and its sensitivity is at its maximum. Even where **a** $/t_c \leq 1/5$, a sensitivity three times higher than in pure PZT can be gained [7]. It is evident that the condition **a** $/t_c << 1$ for the best composites places enormous demands on the production of these materials.

3. Theoretical Models for Composites

In this section, the dielectric, elastic, and piezoelectric properties of a composite will be calculated for the case where it can be regarded as a homogeneous medium. These properties will be presented in a form where they can be compared with the experimental data won from common resonance methods [8] in a form which is useful for applications. The properties of composites with 1-3 connectivity (Figure 1, left), of porous ceramics with 3-3 connectivity, and of porous ceramics with 3-0 connectivity and evenly distributed pores with isotropic or anisotropic pore shape (Figure 1, right) are investigated. The latter are interesting because very finely structured porous ceramics can be developed with photolithographic techniques.

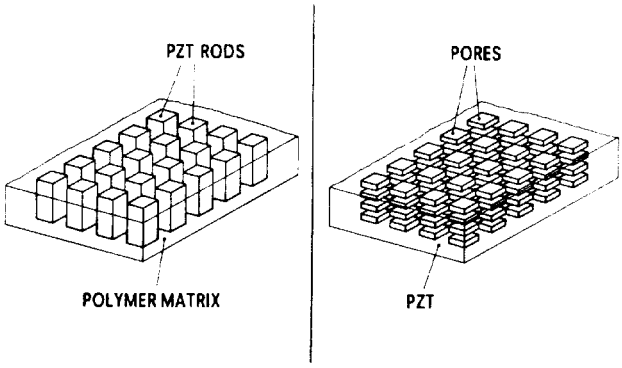

Fig. 1. Schematic representation of a composite and a regular porous ceramic.

3.1 Irregular porous ceramics

Wagners theory [9] allows the calculation of the effective permittivity ε^* of a body that is comprised of a material with permittivity ε'' dispersed in low concentration $v''<<1$ in a material with permittivity ε' (Figure 2). Bruggeman [10] calculated the effective permittivity for arbitrary concentrations v''. Bruggeman similarly calculated the bulk and shear moduli for isotropic materials [11]. The "effective medium approximation" as employed by Marutake [12] for porous ceramics is based on areas of permittivity ε' which are dispersed in the effective medium with permittivity ε^* (Figure 2). This method gives the same results as Bruggeman's theory. Bruggeman's results can be directly applied to unpoled porous piezoelectric ceramics and this can also be extended to the case of poled ceramics [4]. Since the permittivity of the pores $\varepsilon''=\varepsilon_0$ is much smaller than that of the ceramic $\varepsilon=\varepsilon'$, and since the bulk and shear moduli of the pores equal zero, Bruggeman's equations can be substantially simplified for porous ceramics [4]. For example, for ceramics with 3-3 connectivity, one obtains the simple relation

$$\varepsilon^*(p) = \varepsilon(1-3p/2) \qquad (1)$$

for the effective permittivity ε^* as a function of porosity. This is valid for porosities up to $p \approx 0.6$. Figures 3 to 9 show the results that were found in reference 4 using this theory.

* Newnham [2] introduced the term connectivity for this.

** The first number describes the ceramic's dimension of interconnection, the second the plastic's dimension of interconnection.

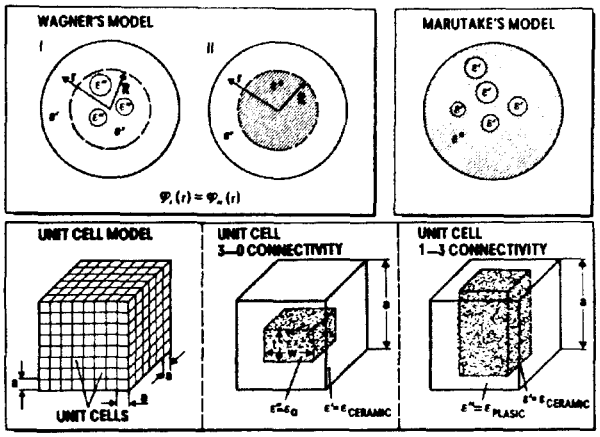

Fig. 2. Models for composites and porous piezoelectic ceramics.

3.2 Regular porous ceramics

In Figure 1, right, the microstructure of a regular porous ceramic is sketched. This ceramic is comprised of cubic cells which all have the same size, as shown in Figure 2. If an electric field or a mechanical force is applied parallel to the edges of the cells, then the average field strength <E>, the average dielectric displacement <D>, the average elastic stress <T> and strain <S> have the same value in each cell. Through calculation of these parameters for one cell, one can obtain the effective material properties $s_{\alpha\beta}^*$, $d_{i\alpha}^*$, and ε_{ik}^* by employing the piezoelectric basic equations.

$$\begin{aligned} <S_\alpha> &= s_{\alpha\beta}^* <T_\beta> + d_{k\alpha}^* <E_k> \\ <D_i> &= d_{i\beta}^* <T_\beta> + \varepsilon_{ik}^* <E_k> \end{aligned} \qquad (2)$$

The porosity p of the ceramic is given by $w^2 t/a^3$.

According to the technique used, the porosity can be varied in a way that either the relative thickness of pores $\tau = t/a$ or the anisotropy $\beta = t/w$ is kept constant. It is reasonable to first calculate the effective material properties for the former case, i.e. as a function of p and τ. By replacing τ with $\tau = p^{1/3} \cdot \beta^{2/3}$, one obtains the results for constant pore shape.

The calculation can be much simplyfied if the case of an unpoled ceramic is taken since the calculation of the effective dielectric and elastic properties is then not coupled. The effective permittivity of a porous ceramic in the pores' thickness direction (3-axis) simply results in

$$\varepsilon_{33}^* = \varepsilon(1-p/\tau) \qquad (3)$$

because $\varepsilon/\varepsilon_0 >> 1$. For the case of polarized ceramics, varying mechanical stresses in the areas around the pores and near their top and bottom cause a varying field distribution. This effect leads to a slight additional reduction in permittivity which peaks at $p=0.4$ and reaches values of about 10%.

The calculation of compliances is shown with the aid of the coefficient s_{33}^D. For the case of mechanical forces in 3-direction (in the thickness direction of the pores), an average mechanical stress $<T_3>$ exists in the ceramic, while the stresses $<T_1>$ and $<T_2>$ are equal to zero. Due to differences in mechanical stress in the area **m** around the pore, and the area **b** above and below the pore, the strains

$$S_\alpha^m = s_{\alpha\beta} T_\beta^m; \quad S_\alpha^b = s_{\alpha\beta} T_\beta^b \qquad (4)$$

will also differ.

For an individual cell, however, the relations

$$S_1^m = S_1^b; \quad S_2^m = S_2^b \qquad (5)$$

are valid.
From $<T_1> = <T_2> = 0$ one finds:

$$T_1^m = -\frac{a(a-t)}{t(a-w)} \cdot T_1^b \qquad (6)$$

$$T_2^m = -\frac{a-t}{t} \cdot T_2^b$$

The stresses in 3-direction are described by:

$$T_3^b = <T_3>; \quad T_3^m = \frac{a^2}{a^2-w^2} \cdot <T_3> \qquad (7)$$

If one applies the Equations (6) and (7) to the Equations (5), one obtains:

$$T_1^a = \frac{w^2 \cdot t}{(a+w)(a^2-tw)} \cdot \frac{s^D_{12}}{s^D_{11}+s^D_{12}} \cdot <T_3> \qquad (8)$$

$$T_2^a = \frac{w^2 \cdot t}{a \cdot (a^2-w^2)} \cdot \frac{s^D_{12}}{s^D_{11}+s^D_{12}} \cdot <T_3>$$

In addition, one obtains using Equation (6), T_1^m and T_2^m as a function of $<T_3>$. This allows, using Equation (4), the calculation of all strains as a funktion of $<T_3>$. From the average strain in 3-direction

$$<S_3> = \frac{t}{a} \cdot S_3^m + \frac{a-t}{a} \cdot S_3^b = s_{33}^{*D} <T_3> \qquad (9)$$

one finally calculates

$$s_{33}^{*D} = s_{33}^D \left[1 + \frac{p}{1-p/\tau} - \frac{\sigma^{D^2}}{1+\sigma^D} \cdot \frac{p \cdot \sqrt{p/\tau} \cdot (1-\tau)}{(1-p/\tau)(1-\sqrt{p \cdot \tau})} \right] \qquad (10)$$

with $\sigma^D = s_{12}^D/s_{11}^D$ being Poisson's ratio for the unpoled ceramic. Because $\langle S_1\rangle = S_1^m = S_1^b$, one obtains:

$$s_{13}^{*D} = s_{13}^D\left[1+\frac{p}{(1+\sigma^D)(1+\sqrt{p/\tau})(1\sqrt{p\cdot\tau})}+\frac{\sigma^D\cdot p}{(1+\sigma^D)(1-p/\tau)}\right] \quad (11)$$

In a similar way, one can calculate the parameters s_{11}^{*D} and s_{12}^{*D} for $\langle T_1\rangle \neq 0$ and $\langle T_2\rangle = \langle T_3\rangle = 0$:

$$s_{11}^{*D} = s_{11}^D\left[1+\frac{p}{1-\sqrt{p\cdot\tau}}-\frac{\sigma^{D2}}{1+\sigma^D}\cdot\frac{\tau\cdot p\cdot(1-\sqrt{p/\tau})}{(1-\sqrt{p\cdot\tau})^2}\right] \quad (12)$$

$$s_{12}^{*D} = s_{12}^D\left[1+\frac{p/(1-\tau)}{1+\sigma^D)(1-\sqrt{p\cdot\tau})^2}+\frac{\sigma^D\cdot p}{(1+\sigma^D)(1-\sqrt{p\cdot\tau})}\right] \quad (13)$$

For pores with cubic shape ($\tau = p^{1/3}$), the results from Equations (10) and (11) equal those from Equations (12) and (13) (isotropic material).

After the effective coupling factors have been calculated, the coefficients $s_{\alpha\beta}^E$ of the poled ceramic can be calculated from the coefficients $s_{\alpha\beta}^D$ of the unpoled porous ceramic, as shown in Ref. 4.

To calculate the piezoelectric moduli, we assume that the electric field strength inside the total cell area surrounding a pore is constant, and that $\langle T_1\rangle = \langle T_2\rangle = \langle T_3\rangle = 0$. From this last condition and assuming equal strain directly above, below and to the side of the pore, one findsequations for the calculation of the elastic stress components $T_1 = T_2$ and T_3 as a function of E_3 in these areas. These equations can be used to calculate the strains in the various areas; from those, the averaged strains $\langle S_1\rangle$ and $\langle S_3\rangle$ and therefore d_{31}^* and d_{33}^* can be calculated.
One finds

$$d_{31}^* = d_{31}\left[1-\frac{p(1-\tau)}{\tau(1-\sqrt{p\cdot\tau})}+f(p,\tau)\right] \quad (14)$$

and

$$d_{33}^* = d_{33}\left[1+p-p/\tau+g(p,\tau)\right]. \quad (15)$$

The correction terms $f(p,\tau)$ and $g(p,\tau)$ in equations (14) and (15) are, in a rather complicated manner, dependent on p and τ, as well as on the ratios s_{12}^E/s_{11}^E, s_{13}^E/s_{11}^E, s_{33}^E/s_{11}^E, and d_{31}/d_{33}. Their influence on the result is small. For example, the effect of $g(p,\tau)$ on the coupling factor k_{33}^* (calculated from d_{33}^*) in the entire range $0\leq p\leq 1$ is less than 2%. For the coupling factor k_{31}^*, the effect of the correction term $f(p,\tau)$ is more noticeable. It causes a faster decrease of k_{31}^* with increasing porosity, e.g. for cubic pores with p=0.8 to values of 0.16 instead of 0.21 without correction.

3.3 Ceramic-plastic composites

Figure 1, left, shows a diagram of the microstructure of these composites, and Figure 2 shows the unit cell used for the calculation of the effective material properties. If **w** is used to denote the width of a ceramic rod embedded in plastic, the volume portion of the plastic is $v^p = 1-(w/a)^2$ which we signify, analogous to porosity in porous ceramics, with p (p=vp).

Since now the electric field strength E_3^c in the ceramic and E_3^p in the plastic equal $\langle E_3\rangle$, the calculation of the material constants can easily be accomplished directly for a poled ceramic. We examine the case where $\langle T_1\rangle = \langle T_2\rangle = \langle T_3\rangle = 0$, and presently disregard lateral stresses in the ceramic and in plastic. Given the conditions (cell model)

$$S_3^c = S_3^p \text{ that means } s_{33}^E\cdot T_3^c + d_{33}\langle E_3\rangle = s_{11}^p\cdot T_3^p$$

$$\text{and} \quad \langle T_3\rangle = 0 = w^2\cdot T_3^c + (a^2-w^2)\cdot T_3^p \quad (16)$$

T_3^c can be calculated as a function of $\langle E_3\rangle$.

With

$$D_3^c = d_{33}\cdot T_3^c + \varepsilon_{33}^T\cdot\langle E_3\rangle,\ D_3^p = \varepsilon^p\cdot\langle E_3\rangle, \quad (17)$$

$$\text{and} \quad a^2\cdot\langle D_3\rangle = w^2\cdot D_3^c + (a^2-w^2)D_3^p \quad (18)$$

we obtain:

$$\varepsilon_{33}^{*T} = \varepsilon_{33}^T\left(1-p\left(1-\frac{\varepsilon^p}{\varepsilon_{33}^T}\right)\right)\left(1-k_{33}^2\frac{s_{33}^E}{s_{11}^p}\cdot\frac{p}{1-p}\right) \quad (19)$$

Since for practically all plastics $\varepsilon^p \ll \varepsilon_{33}^T$ and $s_{33}^E \ll s_{11}^p$, Equation (19) reduces to

$$\varepsilon_{33}^{*T} = \varepsilon_{33}^T\cdot(1-p) \quad (20)$$

Therefore, disregarding lateral stresses was justified.

The calculation of the compliances will be demonstrated using s_{33}^{*E}. We will now examine the case where the field strength in the ceramic is 0, and where $\langle T_1\rangle = \langle T_2\rangle = 0$. Under the last condition, only elastic stresses parallel to the ceramic surfaces occur in the plastic and therefore:

$$(a-w)\cdot T_\parallel^p = w\cdot T_1^c = w\cdot T_2^c$$

$$\text{and} \quad (21)$$

$$S_\parallel^p = S_1^c = S_2^c$$

From the conditions

$$S_3^p = S_3^c = \langle S_3\rangle$$

$$(a^2-w^2)\cdot T_3^p + w^2\cdot T_3^c = a^2\cdot\langle T_3\rangle, \quad (22)$$

two further equations for calculating $T_\parallel^p$, T_3^p, $T_1^c = T_2^c$, and T_3^c as a function of $\langle T_3\rangle$ follow. With these, the strains as a function of $\langle T_3\rangle$ and therefore s_{33}^{*E} can be calculated. Assuming $s_{12}^p/s_{11}^p \approx -1/2$, we find

$$s_{33}^{*} = s_{33}^{E} \cdot \frac{1+\alpha \cdot r}{1-p+\alpha \cdot s} - s_{13}^{E} \frac{q}{p \cdot (1+\alpha q)} \cdot \left[1-(1+\alpha r) \cdot \frac{1-p-2p \cdot \alpha \cdot s_{13}^{E}/s_{11}^{E}}{1-p+\alpha \cdot s} \right]$$

with

$$\alpha = s_{11}^{E}/s_{11}^{p},$$

$$r = 4 \cdot q(1+\sigma^{E})/3$$

$$s = (2/3p)(1+2\sigma^{E}+2s_{33}^{E}/s_{11}^{E}) \qquad (23)$$

$$q = 1/\sqrt{1-p} - 1.$$

For $\alpha \ll 1$ and $p<0.9$, this reduces to:

$$s_{33}^{*E} = s_{33}^{E}/(1-p). \qquad (24)$$

$$\text{With } \langle S_1 \rangle = S_1^{c} \cdot w/a + S_{\perp}^{p} \cdot (a-w)/w \qquad (25)$$

$$\text{and } S_{\perp}^{p} = s_{12}^{p} \cdot (T_{\parallel}^{p} + T_3^{p}), \qquad (26)$$

one obtains for the case $\alpha \ll 1$ and $p<0.9$

$$s_{13}^{*E} = s_{13}^{E} \cdot [u+(1-u)\sqrt{1-p}]/(1-p) \qquad (27)$$

with $u = -(s_{12}^{E}+2s_{33}^{E})/3s_{13}^{E}$.

In a similar way, we find for $\langle T_2 \rangle = \langle T_3 \rangle = 0$ and $\langle T_1 \rangle \neq 0$, the coefficients s_{11}^{*E} and s_{12}^{*E}.
In case $\alpha \ll 1$ and $p<0.9$, we obtain:

$$s_{11}^{*E} = s_{11}^{E} + s_{11}^{p}(1-\sigma p^{2})(1-\sqrt{1-p}) \qquad (28)$$

$$s_{12}^{*E} = s_{12}^{E} + s_{13}^{E} \cdot \sigma p(1-\sqrt{1-p})/\sqrt{1-p} \qquad (29)$$

For calculating the piezoelectric moduli, we consider $\langle T_1 \rangle = \langle T_2 \rangle = \langle T_3 \rangle = 0$. With the conditions $E_3^{c} = \langle E_3 \rangle$, $S_3^{c} = S_3^{p} = \langle S_3 \rangle$, $S_1^{c} = S_2^{c} = S_{\parallel}^{p}$, and $\langle T_1 \rangle = \langle T_3 \rangle = 0$, we calculate $T_1^{c} = T_2^{c}$, T_3^{c}, $T_{\parallel}^{p}$, and T_3^{p} as a function of $\langle E_3 \rangle$. From this we can also calculate $\langle S_3 \rangle$ and d_{33}^{*}. From

$$a \cdot \langle S_1 \rangle = w \cdot S_1^{c} + (a-w) \cdot S_{\perp}^{p} \qquad (30)$$

d_{31}^{*} is calculated. With $d_{31}/d_{33} = -1/2$, we find:

$$d_{31}^{*} = d_{31} \frac{(1-\sigma p)(-\sigma p + (1+2\sigma p)\sqrt{1-p}) + \alpha \cdot f'(p)}{1-\sigma p^{2} + \alpha \cdot h(p)} \qquad (31)$$

$$d_{33}^{*} = d_{33} \frac{1-\sigma p^{2} + \alpha \cdot g'(p)}{1-\sigma p^{2} + \alpha \cdot h(p)} \qquad (32)$$

The correction terms $f'(p)$, $g'(p)$, and $h(p)$ are again dependent on the ratios s_{12}^{E}/s_{11}^{E}, s_{13}^{E}/s_{11}^{E}, and s_{33}^{E}/s_{11}^{E}. With $\alpha \ll 1$, one obtains:

$$d_{31}^{*} = d_{31} \cdot \frac{-\sigma p + (1+2\sigma p)\sqrt{1-p}}{1+\sigma p} \qquad (33)$$

$$d_{33}^{*} = d_{33}$$

The above calculated effective permittivities, compliances, and piezoelectric moduli can now be used [8] to calculate the frequency constant N_1^{*}, Poisson's ratio $\sigma^{*D} = s_{12}^{*D}/s_{11}^{*D}$, the frequency constant $N_{3}^{*}{}_{t}$, the acoustical impedance Z^{*}, and the coupling factors k_{31}^{*} and k_{33}^{*}. The frequency constant of the thickness mode can be calculated for $0.4 \leq k_t^{*} \leq 0.7$ with an error $<3\%$ from

$$N_{3t}^{*} \approx (1/2) \cdot \sqrt{c_{33}^{*E}/\rho^{*}}. \qquad (34)$$

The term c_{33}^{*E} used here is calculated from s_{11}^{*E}, s_{12}^{*E}, s_{13}^{*E}, and s_{33}^{*E}. The density of a porous ceramic can be described through

$$\rho^{*} = \rho(1-p), \qquad (35)$$

of a composite through

$$\rho^{*} = \rho(1-p) + \rho^{p} \cdot p \qquad (36)$$

The parameter

$$Z^{*} = 2 \cdot N_3^{*}{}_{t} \cdot \rho^{*} \qquad (37)$$

describes the acoustical impedance. In addition, the thickness coupling factor k_t^{*} is of interest in ultrasonic transducers. It can be calculated from the effective compliances and the coupling factors [13].

$$k_{33}^{*}{}_{t} = \frac{k_{33}^{*} - C_1 \cdot k_{31}^{*}}{\sqrt{(1-C_1^{2}/C_2)(1-C_2 \cdot k_{31}^{*2})}} \qquad (38)$$

$$\text{with } C_1 = \frac{2 \cdot s_{13}^{*E}}{s_{11}^{*E}+s_{12}^{*E}} \cdot \sqrt{\frac{s_{11}^{*E}}{s_{33}^{*E}}},$$

$$\text{and } C_2 = 2 \cdot s_{11}^{*E}/(s_{11}^{*E}+s_{12}^{*E})$$

The results shown in Figures 3-9 were achieved with the material parameters of a standard piezoelectric ceramic (Vibrit 420 [14]) and those of a plastic having the same elastic properties as PVF_2 (Table 1).

Table 1. Material parameters of Vibrit 420 [14] and PVF_2 [15]

Vibrit 420

s_{11}^E	$15.4 \cdot 10^{-12}$ m²/N	$\varepsilon_{33}^T/\varepsilon_0$	1600
s_{12}^E	$-5.4 \cdot 10^{-12}$ m²/N	k_{33}	0.69
s_{13}^E	$-6.9 \cdot 10^{-12}$ m²/N	k_{31}	0.35
s_{33}^E	$18.7 \cdot 10^{-12}$ m²/N	ρ	$7.7 \cdot 10^3$ kg/m³
		p	≈ 4 %

PVDF

s_{11}^P	$380 \cdot 10^{-12}$ m²/N	$\varepsilon^P/\varepsilon_0$	≈ 10
s_{12}^P	$-165 \cdot 10^{-12}$ m²/N	ρ^P	$1.78 \cdot 10^3$ kg/m³

4. Results and Discussion

4.1 Interpretation of Results

Figures 3 through 9 show the results of our calculations. Material parameters are shown as a function of the material's porosity and as a function of the plastic's volume fraction $v^P=p$ in the ceramic-plastic composite. The figures describe the properties of the following materials:

1. a ceramic-plastic composite with connectivity 1-3 (the following C1); be called in
2. a porous ceramic with irregular porestructure and connectivity 3-3 (material C2);
3. a porous ceramic with regular porestructure and having a cubic shape (material C3);
4. a porous ceramic with regular structure of the pores, where the pores show lamina-like shape (material C4).

In the latter material, either the shape of the pores, (shown in the curves t/w=1/2 and 1/5), or their thickness (thin broken line) is kept constant.

We will view the permittivities first (Figure 3). Because $\varepsilon_0<\varepsilon^P<<\varepsilon$, only the ceramic's dielectric displacement contributes to permittivity. Therefore ε^* will decrease linearly with p in the material C1 and C4 if the thickness of the pores is kept constant (curve t/a=1/5). In materials with constant shape of pores, the cross section of electrical flux is not proportional to p, and therefore ε^* no longer decreases linearly with p. It is interesting that also for an irregular structure of pores (material C2) for $p \leq 0.6$, the permittivity decreases linearly with p, as has been extensively discussed in Reference 4.

Figure 4 shows the frequency constant N_1^* as it is measured on slim rods which vibrate in a length extensional mode perpendicular to polarization and perdendicular to the ceramic rods

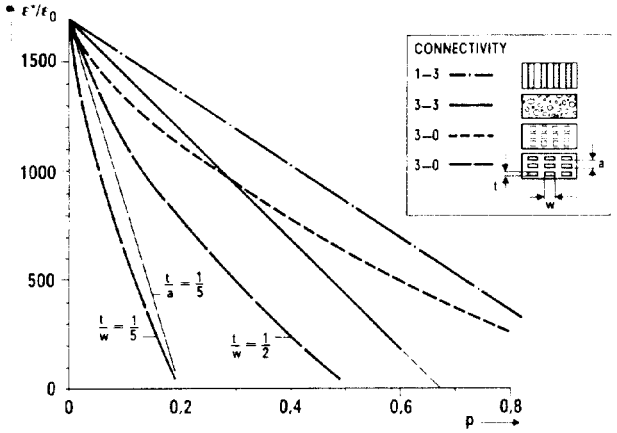

Fig. 3. Permittivity of a composite and of porous PZT ceramics.

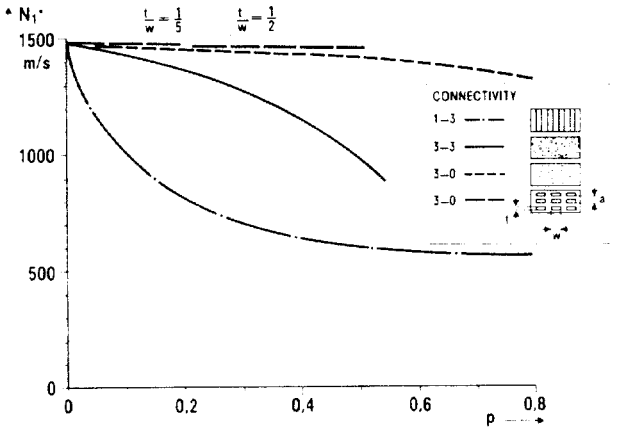

Fig. 4. Frequency constants of a composite and of porous PZT ceramics (length-extensional mode).

in C1, or the pores thickness in C4. It is remarkable that N_1^* decreases quickly even when the volume portion of plastic in C1 is low, but decreases slowly with p in regular porous ceramics. The former is caused by a steep increase of s_{11}^* (because $s_{11}^P>>s_{11}^E$) even at low plastic portions. Not until the plastic reaches higher volume fractions, is this effect compensated by the decreasing density, leading to a decrease in the slope of N_1^*. In contrast, in regular porous materials the increase of s_{11}^* with p is almost completely compensated by the decrease of ρ^*. N_1^* therefore decreases only slowly with p.

With flat pores, (t/w<1) s_{11}^* will increase less with p, leading to a very small decrease of N_1^*. Because of the irregular structure, the compliance of C2 increases faster with increasing porosity, which then terminates in a strong decrease of N_1^*.

The value of Poisson's ratio in ceramic-plastic composites and porous ceramics also show a high difference. The parmeter $|\sigma^*| = |s_{12}^*/s_{11}^*|$ also decreases quickly with p at low volume fractions of plastic p<0.1. This can be attributed to the simultaneous strong increase of

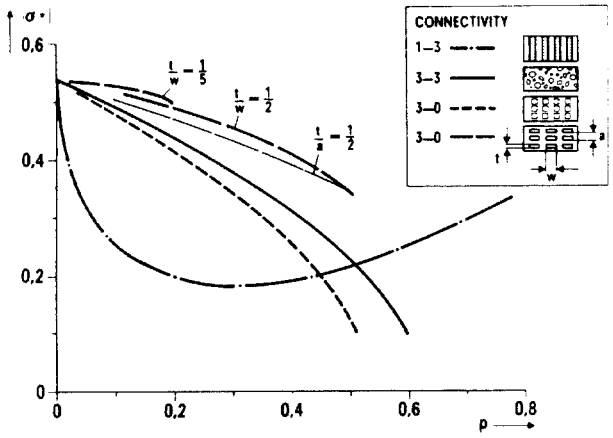

Fig. 5. Poisson's ratio of a composite and of porous PZT ceramics.

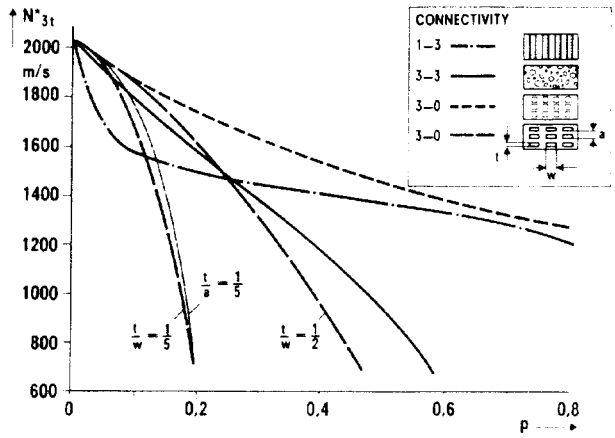

Fig. 6. Frequency constants of a composite and of porous PZT ceramics (thickness mode).

s_{11}^* with p. At medium porosity, the ceramic rods hinder the transverse strain of the plastic. At high porosities this effect diminishes more quickly, and one finally obtains the relatively high value for Poisson's ratio in plastic.

In a material with a cubic shape of pores, $|s_{12}^*|$ decreases slowly with increasing porosity because clamping is caused by the material walls that are perpendicular to the applied forces. This leads, in combination with the increase of s_{11}^* with p to a relatively strong decrease of $|\sigma^*|$ with p. The circumstances are quite different when flat pores are considered. Here $|s_{12}^*|$ increases with p because the areas above and below the pores have to take more strain and because here the transverse stiffness is lower. The increase of s_{11}^* with p therefore causes a small decrease of $|\sigma^*|$ with p. In a similar way the behavior of $|\sigma^*|$ in ceramics with irregular porous structure (C2) can be explained.

The frequency constant $N_3{}^*{}_t$ of the thickness mode is of immediate interest for the transducer design. We will first examine the composite C1. The frequency constant $N_3{}^*{}_t$ decreases quite quickly at low plastic fractions, from the value of a ceramic vibrating in thickness mode down to a value ≈ 1500 m/s, as is often measured for the longitudinal mode. The reason for this is that the plastic layers increasingly reduce the lateral clamping in the ceramic rods. When the volume fraction of plastic reaches p>0.7, $N_3{}^*{}_t$ finally approaches half the value of the sound velocity in plastic. In porous ceramics, the decreases of the frequency constant $N_3{}^*{}_t$ must be explained differently. This follows from the strong increase of s_{33}^* with increasing porosity. If this already occurs at higher porosity σ^* of the material, as is the case with flat pores (e.g. t/w=1/2), one finds a stronger decrease of $N_3{}^*{}_t$ with p. The material C2 can be treated similarly.

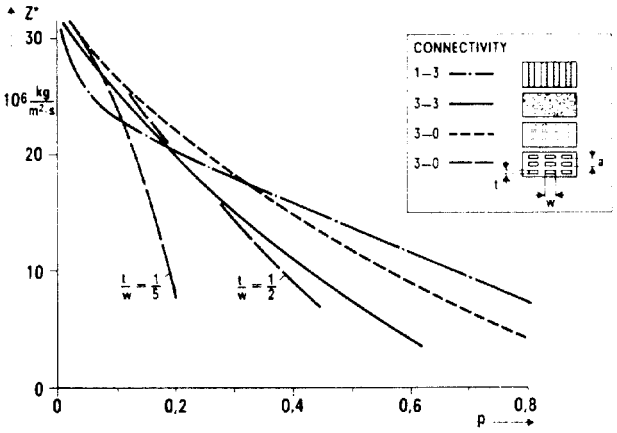

Fig. 7. Acoustic impedance of a composite and of porous PZT ceramics.

The acoustical impedance of the material also is an important device parameter. It is described by Z*, as shown in Figure 7. The numbers immediately follow from Figure 6 and the behavior of σ^* with p.

Figure 8 shows the electromechanical coupling factors of the various materials. The high ratio $s_{11}{}^P/s_{11}{}^E$ causes the piezoelectric coefficient d_{33}^* to practically equal d_{33} in the composite C1. Since an increase in $s_{33}{}^{*E}$ with p just compensates a decrease in $\varepsilon_{33}{}^{*T}$ with p, it follows that $k_{33}{}^* \approx k_{33}$. Although d_{31}^* decreases only slowly with p, k_{31}^* decreases quickly with p even at low plastic fractions because $s_{11}{}^{*E}$ increases correspondingly. The coupling factors of C2 were extensively discussed in Reference 4.

Considering the porous ceramic C3, d_{33}^* first decreases because of mechanical stresses in the ceramic, and later increases at high porosities with p>0.6. This directly influences k_{33}^* because the influence of the $\varepsilon_{33}{}^{*T}$'s and the $s_{33}{}^{*E}$'s dependence on porosity again compensate each other.

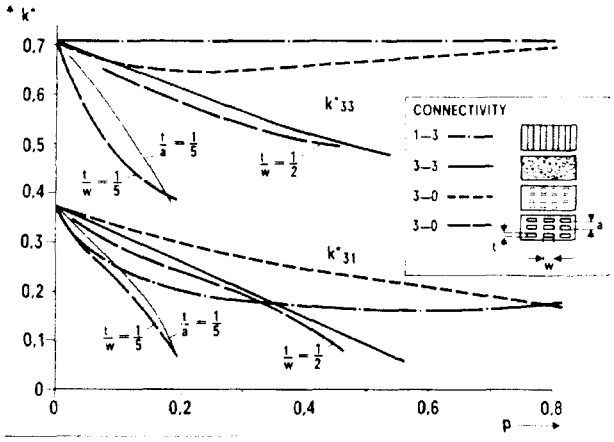

Fig. 8. Effective electromechanical coupling constants k^*_{31} and k^*_{33}.

The decrease of d_{31}^* and k_{31}^* is caused by mechanical stresses in the walls of the ceramic. If the ratio t/w of the pores decreases, the parameters d_{33}^* and d_{31}^* are increasingly reduced by inner elastic stresses.

The thickness coupling factor k_t^* is the third essential device parameter. Its behavior is shown in Figure 9. The coupling factor k_t^* describes the deflection in thickness direction of a laterally clamped sample. The piezoelectric transverse effect causes lateral elastic stresses which reduce the deflection in thickness direction by way of s_{13}^* (see Equation (38)).

This means that in the ceramic-plastic composite C1, that k_t^* rises quickly to values near k_{33}^*, because k_{31}^* decreases quickly with p and because $|s_{12}^*/s_{11}^*|$ as well as $|s_{13}^*/s_{11}^*|$ decrease at the beginning. For porosities higher 0.6, k_{31}^* stays essentially constant, but $|s_{12}^*/s_{11}^*|$ and $|s_{13}^*/s_{11}^*|$ start to increase,

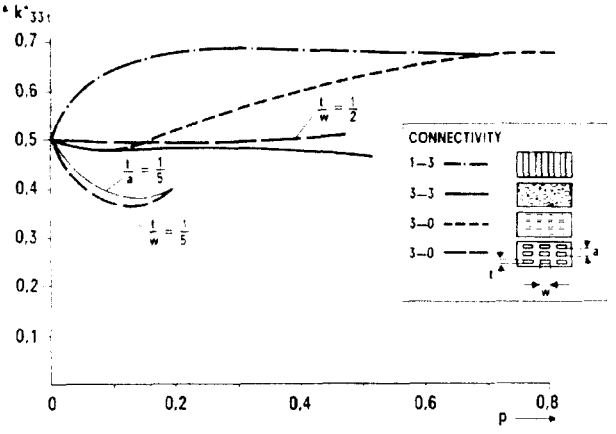

Fig. 9. Effective electromechanical coupling constants k^*_{33t}

resulting in a decrease of k_t^*. The increase of k_t^* in C 3 can be explained in a quite similar way. Naturally, the materials C2 and C4 (t/w=1/2) cannot show an increase of k_t^* because here k_{33}^* decreases with p. It follows then that the behavior of k_t^* in the materials C4 (t/w=1/5) and C4 (t/a=1/5) is essentially determined by the decrease of k_{33}^* with p.

4.2 Experimental verification

A great number of papers on piezoelectric ceramic-plastic composites has been published in recent years. Most of these publications viewed the properties of these materials at low frequencies (see e.g. References 16, 17). There is relatively little data, however, that was won from resonance measurements [18, 19]. One recent paper presents extensive data, but this only for the compositions which are interesting for applications (p=0.7, 0.8 and 0.9). Taking into account the differences between our material and the one presented in Reference 6, there is good agreement for the parameters ε^*, $N_1{}^{E*}$, and N_{3t}^*. The frequency constants in Reference 6 are slightly higher than our values. It seems that $s_{11}{}^P$ of the plastic used is lower than has been assumed in our calculations. The acoustical impedances, and the values of k_{31}^* calculated from k_p in Reference 6, match our results exactly. The theoretically predicted high thickness coupling factors are only reached in very thin samples, i.e. when the ceramic rods can vibrate unhindered. In thicker samples ($a/t_c \approx 1/3$), coupling occurs between the ceramic rods through transverse waves in the plastic. This coupling reduces the deflection of the rods, and so causes a decrease in k_t^* down to values between 0.5 and 0.6 [6]. The calculated high values for k_t^* can therefore only be reached in homogeneous composites ($a/t_c \ll 1$). Measurements in References 18 and 19 also agree well with our calculations.

Measurements of the properties for irregular porous ceramics with 3-3 connectivity were described in Reference 4. It can be seen that the properties of these ceramics behave almost exactly as shown in figures 3-9.

Data on regular porous ceramics with a cubic shape of pores are not known to us. Kahn [20] measured the first data on ceramics with anisotropic pores. It is difficult to compare this data with our results since important parameters are still missing. Our first results of measurements on samples with anisotropic pores are shown in Table 2. The samples were produced by a technique as described in the following.

These measurements agree very well the predicted values.

Table 2. Measured properties of piezoelectric ceramics with anisotropic pores

t/a	≈1/5	N_l	1470 m/s
p	≈0.11	N_{3t}	1640 m/s
$\varepsilon/\varepsilon_0$	850	Q_l	60
k_{3l}	0.21	Q_t	15
k_{33t}	0.43		

4.3 Discussion of the results

In this section our results will be discussed in view of the application of various composites for ultrasonic antennas in medical diagnostic devices.

We will start with the acoustical impedances of the varying materials, since, as mentioned in the introduction, its high value in piezoelectric ceramics is a decisive disadvantage in these materials. Figure 7 demonstrates that no shown material is suited for an immediate acoustical adaption to human tissue. On the other hand, it is obviously possible to reach acoustical impedances of $8 \cdot 10^6$ kg/m^2•s in all materials. It is necessary though, that the anisotropy of pores in porous ceramics not be too high. With this value of the acoustical impedance, only one adaption layer allows a sufficient adaption of the ultrasonic transducer in a wide frequency range at high sensitivity. For a further comparison of the materials' properties it is reasonable to view the data at those p-values where the acoustical impedances equal $8 \cdot 10^6$ kg/m^{2}s.

At this impedance, the frequency constant for the composites C1 and C3 equals about 1300 m/s, and for C2 and C4 about 900 m/s. This means that the thickness t_c of a 3 MHz transducer is in the first case about 0.45 µm, in the second case about 0.3 µm. If we strive after a material which is as homogeneous as possible, e.g. with an internal structure of period $a \approx (1/5)t_c$ (high sensitivity [7]), the first case leads to $a \approx 90$ µm. This means that the diameter of the individual ceramic rods in the material C1 is about 45 µm (p≈0.75). Even if we allow $a = (1/3)t_c$ - the material cannot be called homogeneous yet, and k_t^* equals only about 0.5 - the ceramic rods must not be thicker than 75 µm. It is obvious that high requirements for the production technology of composites exist even if ultrasonic transducers operating at only 3 MHz are considered. The requirements are even higher for the material C4 ($a \approx 60$ µm). One does not expect these problems, however, in materials with irregular porous structure (material C2).

The thickness coupling factors of the various composites with $Z^* = 8 \cdot 10^6$ kg/m^{2}s will be compared next.

We expect excellent values for k_t^* of about 0.65 in the composites C1 and C3. It is necessary, though, that the above mentioned condition for homogeneity is fulfilled. Even at a $a/t_c = 1/3$ the effective thickness coupling factor reduces to about 0.5 [6]. Since in C1 finer detailed structures cannot be attained today, the material C2 and C4 (t/w=1/2) offer an equally high coupling factor. It should be mentioned though that in ceramics with anisotropic pores, coupling decreases with increasing anisotropy of the pore shape. For this reason, a ratio t/w=1/3 is desired.

The comparison of electrical and mechanical losses in the various materials shows that these values are low enough to allow high sensitivities ($\tan\delta < 0.05$, $Q_m > 10$). In addition, the quality factor Q_m with values between 10 and 20 is low enough, so that a high bandwidth and a fast decay of pulses can be gained. The low quality factors of C1 were, for example, measured in Reference 6, those of C2 in Reference 4.

Measurements on regular porous ceramics show that the quality factor in thickness mode is low for these ceramics. The increase of mechanical losses with increasing frequency (Table 2) indicate Rayleigh scattering of ultrasonic waves at the pores [4].

It is interesting that the effective permittivities of the composites C1, C2, and C3 at the acoustical impedance $8 \cdot 10^6$ kg/m^{2}s equal each other, and that the value of $\varepsilon/\varepsilon_0 \approx 500$ seems suited for application. The permittivity of the material C4 is definitely lower. This does not cause any essential problem, since the permittivity of the starting material PZT can be chosen in wide ranges. Therefore all the mentioned materials allow good electrical adaption.

The comparison of the properties of the four composites (C4 with $t/w \approx 1/2$) showed that they are all equally suited for ultrasonic antennas. Ceramic-plastic composites, however, with their present imperfect homogeneity (i.e. with $a/t_c \approx 0.5$-0.75), offer one advantage [21]. Coupling between the ceramic rods is so low that array elements can be defined solely by electrode patterning [22]. This yields similar conditions as in sash sawed arrays. With increasing homogeneity of the composites (decreasing a/t_c), coupling between the ceramic rods increases [6]. The advantage is then probably lost.

5. Technological Aspects

A great number of methods for producing a vast variety of composites became known in recent years. The most widely used methods for producing composites with 1-3 connectivity have been described by Klicker et al. [16] and by Takeuchi [22]. According to the method of Klicker, PZT rods are extruded and fired. Fired rods (typical diameter ≈ 0.28 mm) are aligned using an array of appropriately spaced holes drilled in a pair of brass discs bolted parallel to each other. Then the

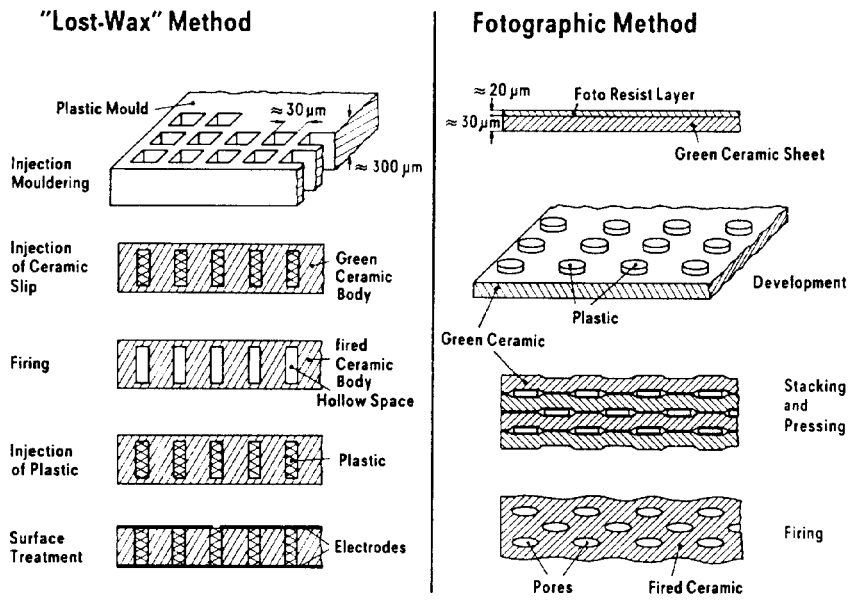

Fig. 10. Structuring of piezoelectric ceramics.

rods are cast in plastic. The desired samples are sawed from these produced blocks and then lapped. Takeuchi's method is quite similar to the sash sawing of today's arrays. Ceramic platelets are sash sawed in the x- and in the y-direction. The PZT-pillars (typically 0.1x0.1 mm^2) are then filled with polyurethane. The two methods have in common that their realization becomes the more difficult, the smaller the desired structures are. Therefore one tries to find a technique which avoids the complicated steps in handling and manufacturing detailed structures. A possible technique, which is being investigated in our laboratory, is shown in Figure 10, left. It is based on our method for production of high quality ceramic foils. A plastic foil, structured in the desired way, is set in vacuum and there cast with ceramic slip. The plates are dried and the plastic is burnt out at relatively low temperatures. After that, the plates are fired, then filled with plastic again, and finally lapped on both sides until they have reached the desired thickness. Doing this, the fine ceramic rods become separated. The parts can be electroded and poled by the usual methods.

A number of techniques to produce porous ceramics have been described in reference 4. For the production of ultrasonic transducers, only those methods that allow for a sufficiently detailed microstructure are suitable. It can be demonstrated that methods based on the above-mentioned technique of foil casting are advantageous for the production of porous ceramics. Very finely structured ceramics with irregular pores can be made by mixing plastic pellets into the ceramic slip or into the ceramic powder [4]. Especially fine and regular internal structures of any shape can be produced by a combination of foil casting and photolithography which is employed in semiconductor technology. In the simplest case, one can produce porous ceramics with regular structure of pores. Figure 10, right shows schematically how to proceed. Green ceramic foils are coated with photo resist or with a plastic foil that can be structured by photolithography. Then the desired pattern is transfered to the photo resist by an exposure process. After development, the desired plastic structure - in the simplest case small discs - remains on the ceramic foil. Coated green foils are stacked and pressed at elevated temperatures. Figure 11 shows a section through a foil stack comprised of 8 ceramic green foils. The variation in thickness of the plastic discs can be attributed to a low stacking accuracy. After the plastic has been burnt out during a defined temperature programm in controlled atmosphere, the samples are fired in a conventional way. Figure 12 shows REM micrographs of a fired sample. The left part of

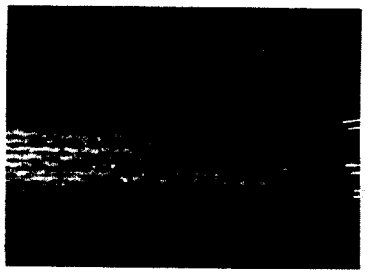

Fig. 11. Photolithographic method for production of porous ceramics.

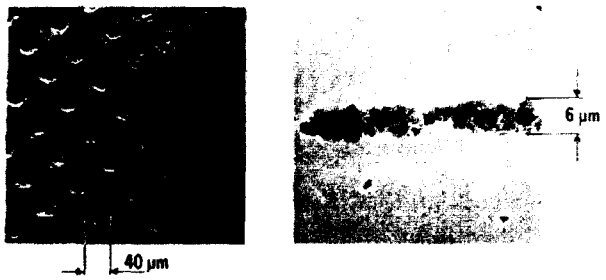

Fig. 12. Microstructure of pores.

Figure 12 shows the pores in one layer as they have been lapped by different amounts, the right part shows a cross section of a pore.

6. Conclusion

For PZT-plastic composites with 1-3 connectivity, for porous ceramics with irregular porous structure and 3-3 connectivity, and for regular porous ceramics with 3-0 connectivity and anisotropic pores, the applicability to ultrasonic antennas fo medical diagnostic devices was investigated. For this, the electromechanical properties of these composites were calculated dependent on the plastic's volume fraction or the amount of porosity. It was shown that all these materials can basically fulfill the requirements for the application as ultrasonic transducers. Since in all cases, acoustical impedances down to $8 \cdot 10^6$ kg/m^{2}s can be attained, one adaption layer suffices for the matching to human tissue. Thickness coupling factors of about 0.5 are obtainable. Possible higher theoretical values for ceramic-plastic composites can only be realised with extremly fine structured composites. Regular porous ceramics with a cubic shape of pores also offer very high effective thickness coupling factors. This, however, decreases with increasing anisotropy of the pores' shapes. The ratio of a pore's width and height should not exceed the value 3.

An advantageous method to produce very finely structured porous ceramics with anisotropic pores uses green ceramic foils which are coated with a photoresist layer, and can be structured by an exposure process.

Acknowledgement

The author is indebted to Dr. U. Bast for his contributions in fabrication of samples and measurements.

References

[1] J. Borburgh, I. Feigt, P, Hini and V. Zurinski, "Bildqualität bei Ultraschallgruppenantennen für die medizinische Realzeitdiagnostik", Siemens Forsch.- u. Entwickl.-Ber., vol.9, pp. 116-119, 1980.

[2] R. E. Newnham, D. P. Skinner and L. E. Cross, "Connectivity and piezoelectric-pyroelectric composites", Mater. Res. Bull., vol. 13, pp. 525-536, 1978.

[3] R. E. Newnham, L. J. Bowen, K. A. Klicker and L. E. Cross, "Composite piezoelectric transducers", Materials in Engineering, vol. 2, pp. 93-106, 1980.

[4] W. Wersing, K. Lubitz and J. Mohaupt, "Dielectric, elastic and piezoelectric properties of porous PZT ceramics", Ferroelectrics, 1986, in print.

[5] Y. Wang and B. A. Auld, "Acoustic wave propagation in one-dimensional periodic composites", in Proc. 1985 IEEE Ultrasonics Symposium, 1986, pp. 637-641.

[6] T. R. Gururaja, W. A. Schulz, L. E. Cross, R. E. Newnham, B. A. Auld and Y. J. Wang, "Piezoelectric Composite materials for ultrasonic transducer applications. Part I: Resonant modes of vibration of PZT rod-polymer composites", IEEE Trans. on Sonics and Ultrasonics, vol. SU-32, pp. 481-498, 1985.

[7] - "Part II: Evaluation of ultrasonic medical applications", IEEE Trans. on Sonics and Ultrasonics, vol. SU-32, pp. 499-513, 1985.

[8] "IRE standards on piezoelectric crystals: Measurements of piezoelectric ceramics", Proc. IRE, vol. 49, pp. 1161-1169, 1961.

[9] K. W. Wagner, "Erklärung der dielektrischen Nachwirkungsvorgänge aufgrund Maxwell'scher Vorstellungen", Arch. Elektrotechn., vol 2, pp. 371-387, 1914.

[10] D. A. G. Bruggeman, "Berechnung verschiedener physikalischer Konstanten von heterogenen Substanzen. I. Dielektrizitätskonstanten und Leitfähigkeit der Mischkörper aus isotropen Substanzen", Ann. Phys. Lpz., vol. 24, pp. 636-664, 1935.

[11] - "III. Die elastischen Konstanten der quasiisotropen Mischkörper aus isotropen Substanzen", Ann. Phys. Lpz., vol 29, pp. 160-178, 1937.

[12] M. Marutake and T. Ikeda, "Elastic constants of porous materials, especially of $BaTiO_3$ ceramics", J. Phys. Soc. Jap., vol. 11, pp. 814-818, 1956.

[13] W. Wersing, to be published.

[14] Siemens AG, Kunststoff- und Porzellanwerk Redwitz, VIBRIT Piezoelectric Ceramic Catalogue.

[15] R. H. Tancrell, D. T. Wilson and D. Ricketts, "Properties of PVF_2 polymer for sonar", in Proc. 1985 IEEE Ultrasonics Symposium, 1986, pp. 624-629, 1986.
[16] K. A. Klicker, J. V. Biggers and R. E. Newnham, "Composites of PZT and epoxy for hydrostatic transducer applications", J. Amer. Ceram. Soc., vol. 64, pp. 5-8, 1981.
[17] K. A. Klicker, W. A. Schulze and J. V. Biggers, "Piezoelectric composites with 3-1 connectivity and a foamed polyurethane matrix", J. Amer. Ceram. Soc., vol. 6, pp. C208-C210, 1982.
[18] T. R. Gururaja, W. A. Schulze, T. R. Shrout, A. Safari, L. Webster and L. E. Cross, "High-frequency applications of PZT-polymer composite materials", Ferroelectrics, vol. 39, pp. 1245-1248, 1981.
[19] T. R. Gururaja, W. A. Schulze and L. E. Cross, "Resonant modes of vibration in piezoelectric PZT-polymer composites with two-dimensional periodicity", Ferroelectrics, vol. 54, pp. 183-186, 1984.
[20] M. Kahn, "Acoustic and elastic properties of PZT ceramics with anisotropic pores", J. Am. Ceram. Soc., vol 68, pp. 623-628, 1985.
[21] C. Nakaya, H. Takeuchi, K. Katakura and A. Sakamoto, "Ultrasonic probe using composite piezoelectric materials", in Proc. 1985 IEEE Ultrasonics Symposium, 1986, pp. 634-636.
[22] A. Shaulov and W. A. Smith, "Ultrasonic transducer arrays made from composite piezoelectric materials", in Proc. 1985 IEEE Ultrasonics Symposium, 1986, pp. 648-651.
[23] H. Takeuchi and C. Nakaya, "PZT-polymer composite for medical ultrasonic probes", to be published in Ferroelectrics.